A New Flame Monitor With Triple Photovoltaic Cells

Lijun Xu, *Senior Member, IEEE*, and Yong Yan, *Senior Member, IEEE*

***Abstract*—In this paper, we present a new flame monitor that uses three photovoltaic cells covering the ultraviolet (UV), visible, and infrared (IR) spectral bands. A gain-adjustable amplifier is incorporated into the monitor so that it is applicable to the coal-, oil-, or gas-fired flames. Self-checking of the monitor is implemented through cross correlation of the signals from the three cells, and hence, no additional self-checking hardware is required. Both the oscillation frequency and the brightness of the flame are used to monitor flame stability and to detect flame presence as well as sighting-tube blockage. Unlike conventional single-cell flame detectors, the new multicell devices can still be in operation before being repaired, after a cell-failure alarm has gone off. Experiments were carried out on an industrial-scale combustion test facility in order to demonstrate the operability and efficacy of the new flame monitor.**

***Index Terms*—Combustion safety, cross correlation, flame monitor, flame stability, industrial boiler.**

I. Introduction

SAFE operation of an industrial boiler depends on a stable combustion of fuels. Unstable flames can be both inefficient and pollutant forming, but, in extreme cases, flame extinction can occur. A flame-monitoring device is installed on a burner primarily for safety reasons [1]. Most flame monitors use low-cost but reliable sensors, and some have been applied to indicate the flame stability. Although thermocouples, heat-flux meters [2], nonintrusive pressure transducers [3], and acoustic devices [4] for flame monitoring were studied and applied in the early years, optical monitors based on radiation detection have been recognized as the most successful.

The optical flame monitors can be classified into two categories: brightness and oscillation-frequency monitors. The brightness monitors can be further classified into infrared (IR), visible, and ultraviolet (UV) groups, according to their working spectral bands. As brightness monitors using the visible and IR regions of the electromagnetic spectrum can be affected by the radiation from the neighboring burners and hot refractory or water walls, they are now seldom used. The UV monitors can overcome this problem, as most flames produce the UV radiation only in the zone of the initial combustion. The furnace temperature is so low that the furnace walls and the combustion products do not normally generate the UV emission. The main problem with this type of monitor is that the unburned fuel in the flame skirt, smoke, airborne dust, and dirt, or the deposits on the flame-sighting-tube lens can attenuate the UV signal reaching the cell. Clean conditions are, therefore, essential for a satisfactory operation of such monitors. The oscillation-frequency monitors are often of the visible or IR types, as they use only the oscillatory signals of a flame, ensuring that they ignore the steady-state radiation from the hot refractory, slag buildup, etc. Early monitors of this type are only sensitive to the low-frequency fluctuating signals from 10 to 30 Hz. As such low-frequency signals are easily picked up anywhere in a furnace, this type of system is now seldom used. Modern commercial flame monitors combine both the brightness and high-frequency oscillatory signals for an improved reliability.

All the above monitors use a single photovoltaic cell only. A separate self-checking mechanism is therefore necessary to ensure the cell is working properly. However, the extra-checking mechanism may also be another source of a monitor failure. Although the cross-correlation-based system uses two optical cells [5], it requires two separate optical paths and a separate self-checking unit for each cell. Monitors of this type are seldom used in modern boilers.

In this paper, a new flame monitor is presented, which consists of three photovoltaic cells covering the UV, visible, and IR spectral bands. The cross correlation between the three signals from the cells is deployed to achieve self-checking of the sensor, and hence, no dedicated self-checking hardware is required. Both the oscillation frequency and the brightness of the flame are used to monitor the flame stability and to detect the flame presence and sighting-tube blockage.

II. System Structure

The combustion flames radiate energy in a continuous band, but of varying intensity from the UV through the visible spectrum to the far IR [6]. Oil and pulverized fuel flames may look more reddish compared to the bluish gas flames. Majority of the burners in the industrial boilers have flame sighting tubes preinstalled, aiming at the zone of the initial combustion. Fig. 1 shows a typical installation arrangement of the sighting tube. A new flame monitor with the same installation specifications has been designed. The schematic diagram of the new monitor is shown in Fig. 2. The three separate photovoltaic cells covering the UV, visible, and IR regions, collectively, are used to detect the flame-radiation signals. While the spectral response of the visible and IR cells covers the visible and IR bands, respectively, the UV-enhanced cell covers the UV, visible, and IR three bands.[1] Table I summarizes the technical

[1]When the flame under inspection goes out, no UV radiation can be detected, and the signal from a pure UV-sensitive cell may be irrelevant to the visible and IR signals, resulting in a very small correlation coefficient that is unwanted for the monitor self-checking through cross correlation. Therefore, a UV-enhanced cell is adopted here.

Manuscript received June 15, 2005; revised April 19, 2006.

L. Xu is with the School of Instrument Science and Opto-Electronics Engineering, Beijing University of Aeronautics and Astronautics, Beijing 100083, China.

Y. Yan is with the Department of Electronics, University of Kent, Canterbury, CT2 7NT Kent, U.K. (e-mail: y.yan@kent.ac.uk).

Digital Object Identifier 10.1109/TIM.2006.876589

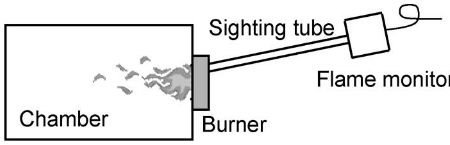

Fig. 1. Typical installation arrangement of the sighting tube.

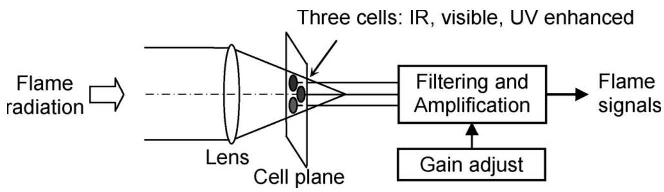

Fig. 2. Schematic diagram of the triple-cell flame monitor.

TABLE I
SPECIFICATIONS OF THE THREE PHOTOVOLTAIC CELLS

Photodiode	Visible	UV enhanced	IR
Model type	OSD1-E	OSD1.2-7U	X55-754
Wavelength range (nm)	350-800	190-400	850-1700
Peak wavelength (nm)	550	230 and 340	1550
Rise time (ns)	7	100	0.3
Capacitance (pf)	6-30	40	1.5
Dark current (nA)	0.5-2	0.002	3
Operation temperature (°C)	-25 ~ +75	-55 ~ +70	-40 ~ +100
Responsivity	1 nA/Lux	0.1 A/W@254nm 0.15 A/W@340nm	0.9 A/W

specifications of the three photovoltaic cells. A quartz lens is used to collect the flame radiation optically. The diameter and the focus of the lens are 25 and 30 mm, respectively. The detection plane of the three photovoltaic cells is 18 mm away from the lens plane. The weak current induced on each cell is amplified via an in-house designed amplifier (LF347) with a high input resistance. A second-order lowpass filter with the cutoff frequency adjustable within 1–5 kHz was used for each cell in the amplifier to remove the high-frequency noise. As the spectral distribution of the flame radiation may vary with the boiler (type and capacity) and fuel type, a gain-adjustable unit is incorporated in the monitor to ensure its applicability to a wide range of the combustion conditions.

III. PRINCIPLES

A. Self Checking

As the three cells aim at the same point of a flame, the three flame signals obtained are correlated. Therefore, the cross-correlation technique can be used to diagnose the working condition of each cell. If one of the three cells develops a fault, the cross correlation involving the signal from this cell will give rise to a small correlation coefficient. However, the cross correlation of the two signals from the two working cells yields a high level of correlation coefficient, provided the flame is under the normal conditions.

Let $\{x(n)|n = 0, 1, \ldots, N-1\}$ and $\{y(n)|n = 0, 1, \ldots, N-1\}$ denote the two samples obtained from any two cells, with N being the sample length. The normalized cross-correlation function of the two samples is given by

$$r(k) = \frac{\sum_{n=0}^{N-1} [(x(n) - \overline{x}) \cdot (y(n+k) - \overline{y})]}{\sqrt{\sum_{n=0}^{N-1} [x(n) - \overline{x}]^2} \cdot \sqrt{\sum_{n=0}^{N-1} [y(n) - \overline{y}]^2}} \tag{1}$$

where $\overline{x}$ and $\overline{y}$ are the mean values of the two samples. In this research, $r(0)$ is referred to as the correlation coefficient between the two samples and ranges between -1 and 1. If $r(0) = 1$, then the two signals are perfectly identical. The greater is the correlation coefficient, the more similar are the two signals.

If all of the three cells work properly, a combination of any pair of the three signals should produce a high level of correlation coefficient. Therefore, a lower limit of the correlation coefficient $r_{\min}$ is set as a threshold so that an alarm will be triggered if the correlation coefficient goes below the threshold. It is also possible to pick out the faulty cell. Let cell 1, cell 2, and cell 3 represent the IR, visible, and UV extended cells, respectively, and S_1, S_2, and S_3 denote the three corresponding signals. As the three cells are of the different types and work independently, it is very rare for all or any two of them to develop a fault simultaneously. If the correlation coefficient between S_1 and S_2 is below the threshold, either cell 1 or cell 2 develops a fault. Furthermore, if the correlation coefficient between S_1 and S_3 is also below the threshold, it can be concluded that cell 1 is faulty; otherwise, cell 2 is defective. If any two cells develop a fault simultaneously, all of the three correlation coefficients are below the threshold. Although the brightness and the oscillation frequency can be used to pick out the working cell if not all three cells are in faulty conditions, more attention should be paid to identify the reasons why two or three cells develop a fault simultaneously. For example, excessively high environment temperature and power siege could be the two potential factors.

Let r_{12}, r_{13}, and r_{23} denote the correlation coefficients between S_1, S_2, and S_3, and r_{12}^{L}, r_{13}^{L}, and r_{23}^{L} stand for the lower limits of r_{12}, r_{13}, and r_{23}, respectively. The possible decisions for a self-checking are listed in Table II. Once r_{12}, r_{13}, and r_{23} are obtained from the acquired flame signals, the working condition of each cell can be deduced according to Table II.

TABLE II
DECISION TABLE FOR SELF-CHECKING

$r_{12} \leq r_{12}^L$?	$r_{13} \leq r_{13}^L$?	$r_{23} \leq r_{23}^L$?	Self-checking decision
No	No	No	No failures
No	No	Yes	-
No	Yes	No	-
No	Yes	Yes	Cell 3 failure
Yes	No	No	-
Yes	No	Yes	Cell 2 failure
Yes	Yes	No	Cell 1 failure
Yes	Yes	Yes	Two or three cells failures

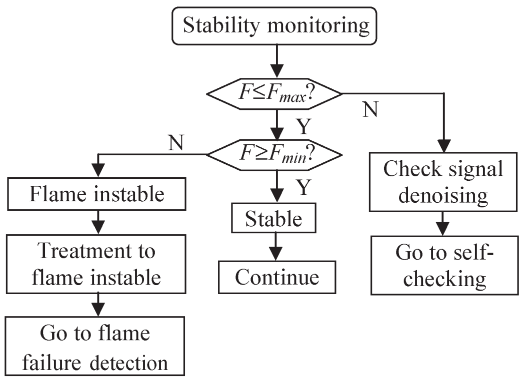

Fig. 3. Algorithm for flame-stability monitoring.

B. Flame-Stability Monitoring

The oscillation frequency of a flame reflects the geometrical pulsation of the flame and the oscillatory nature of the heat radiation and pressure. It is known that the oscillation frequency of a flame is associated with the combustion efficiency and the pollutant emissions [7]–[9]. As an essential attribute of a flame, its oscillation frequency is widely used as an indicator of the flame stability [10], [11]. The oscillation frequency of a flame is defined as the weighted average frequency over the entire frequency range, and the weighting factors are the power densities of the individual frequency components [12]:

$$F = \frac{\sum_{m=1}^{M} [P(m) \cdot f(m)]}{\sum_{m=1}^{M} P(m)} \tag{2}$$

where $P(m)$ is the power density of the mth frequency component $f(m)$ of the flame signal, and M is the total number of frequency components.

However, a flame signal acquired from an industrial boiler often contains a white noise, and the oscillation frequency calculated from (2) is seriously affected by the noise level and the sampling rate. An improved algorithm that uses the wavelet-denoising and adaptive spectrum-truncation techniques has been developed [13] to remove the influence of the white noise and the sampling rate. The algorithm has been proved effective by using the flame signals from an industrial-scale combustion test facility. The improved algorithm is incorporated in the new monitor.

If the flame is stable, its oscillation frequency is within a certain range. When the flame becomes unstable, the lower frequency components become greater and the higher frequency components become weaker, resulting in a reduced oscillation frequency. If the oscillation frequency reaches the lower limit of its normal range, an unstable flame is indicated. If the oscillation frequency exceeds the upper limit of its normal range, this often means that the white noise dominates the signal throughout the signal spectrum and a denoising procedure should be adopted [13]. If the lower and upper limits of the oscillation frequency for a stable flame are given by $F_{\min}$ and $F_{\max}$, respectively, the flame-stability monitoring algorithm can be described in a flowchart, as shown in Fig. 3.

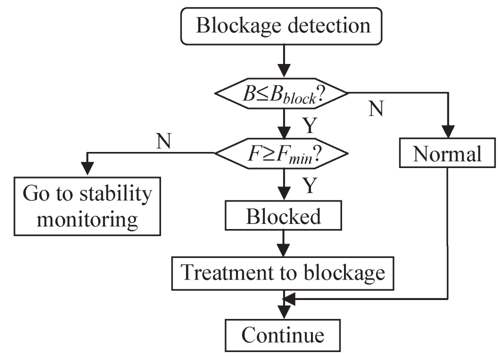

Fig. 4. Algorithm for sighting-tube-blockage detection.

C. Detection of Sighting-Tube Blockage

If the sighting tube (including the monitor lens) is partially blocked by the dirt or deposits, insufficient light will reach the cells resulting in a reduced brightness level (represented by the dc level of each sample). As all the frequency components of the flame signal are attenuated simultaneously, the oscillation frequency does not change significantly unless the extent of the blockage is so great that the white noise dominates each flame signal. Therefore, if the oscillation frequency is within the normal range, but the brightness level goes below a preset threshold, a sighting-tube-blockage alarm should be triggered. This alarm indicates that the monitor will soon fail unless the sighting path is cleaned.

Let B and B_{block} be the brightness level and the blockage threshold, respectively. The algorithm implementing sighting-tube-blockage detection is shown in Fig. 4.

D. Flame-Failure Detection

Both the brightness and flicker signals obtained from the UV-enhanced cell are used to detect the flame failure. If the flame under inspection goes out, the light radiation reaching the optical cell comes from the hot-refractory water walls or flame skirt of the other burners. In this case, no UV radiation can reach the monitor, and the detected radiation in the visible and IR ranges becomes weak too. Therefore, the brightness signal obtained from the UV-enhanced cell is very low in comparison with a flame-on brightness signal. If there is only one burner in the boiler, the flame signal detected when the flame goes out is almost a dc signal, and the oscillation frequency is very close to zero. If there is more than one burner in the boiler, things will be different. Regardless of whether the signal detected by the cell is the reflection and radiation from the hot-refractory or from the hot-furnace water walls or the radiation from the flame skirt of the other burners, the high-frequency components are very weak, and hence, the oscillation frequency is very low. Therefore, if both the brightness and the oscillation frequency are a lot lower than the lower limits of their normal ranges (one third of the normal value or less), it can be certain that the flame goes out.

Let B_{fail} and F_{fail} be the brightness and oscillation-frequency thresholds, respectively, for flame-failure detection. The algorithm for the flame-failure detection is illustrated in Fig. 5.

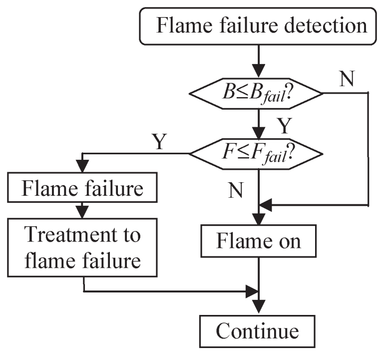

Fig. 5. Algorithm for flame-failure detection.

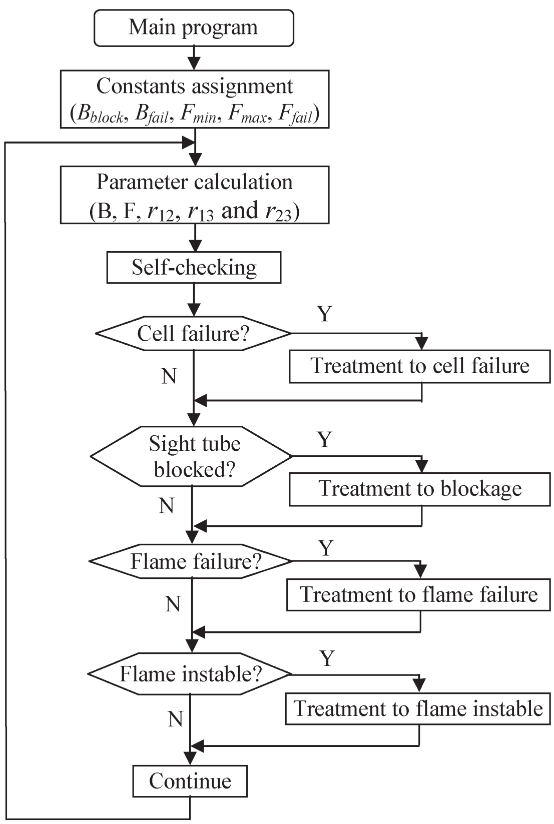

Fig. 6. Main program.

E. Main Monitoring Algorithm

The main monitoring algorithm is shown in Fig. 6. It should be noted that all the constants need to be determined based on the on-site combustion conditions and sufficient tolerance should be set for each constant.

IV. Initial Experimental Results

The new monitor has been evaluated on a 0.5 MW_{th} pulverized-coal-fired-combustion test facility. The optical cells were all set to aim at the root area of the flame, but at the hot-refractory wall when the flame went out. To shut down the facility, the fuel was gradually changed to propane after the air and fuel flows were reduced to their expected levels. At the early stage of the fuel changeover, special operations were introduced to obtain an unstable flame. Before the introduction of an unstable flame, the flame was kept stable. A metal ring

TABLE III
Indexes of Samples Obtained Under Various Test Conditions

Sample index	Flame status			UV cell failure
	Stable	Unstable	Out	
Sighting tube blocked	1-50	-	-	-
Sighting tube normal	51-100	101-150	151-200	201-250

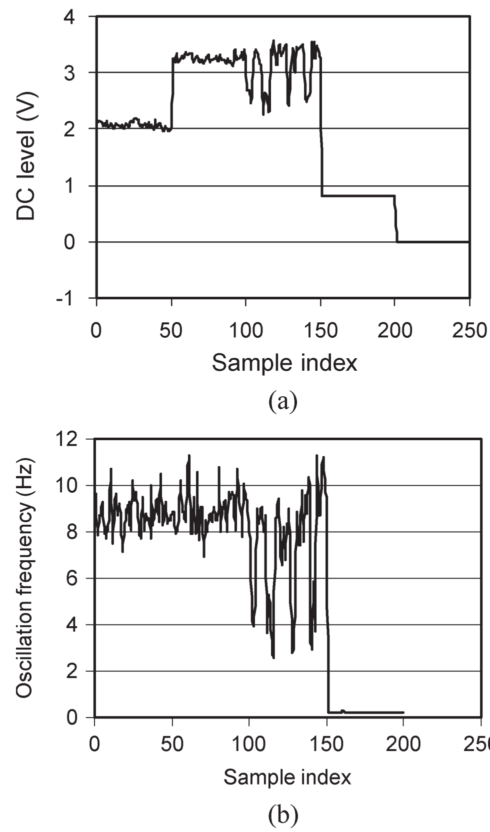

Fig. 7. Brightness and oscillation frequency of the flame (given by the UV-enhanced cell). (a) Brightness and (b) oscillation frequency.

was put in front of the lens of the monitor to create a condition of sighting-tube blockage. In addition, the UV-enhanced cell was removed to create a complete cell-failure condition.

A total of 50 samples of the flame signal were obtained under each of the above conditions. The indexes of the signal samples are listed in Table III. Detailed calculations have shown that the confidence level was greater than 99% if the sampling rate was over 800 Hz [13]. The sampling rate and the sample length used in this study were 1600 Hz and 4096, respectively. Frequency components higher than 800 Hz were treated as noise. The brightness and the oscillation frequency of the flame calculated from the 250 samples obtained from the UV-enhanced cell are plotted in Fig. 7. The variation of the correlation coefficient between the IR and the UV-enhanced signals, with the sample index, is shown in Fig. 8.

The following were observed under the various test conditions.

1) If the sighting tube is blocked, the brightness is reduced, but the oscillation frequency of the flame and the correlation coefficient are similar to their normal values, which are around 9 Hz and 0.9, respectively.

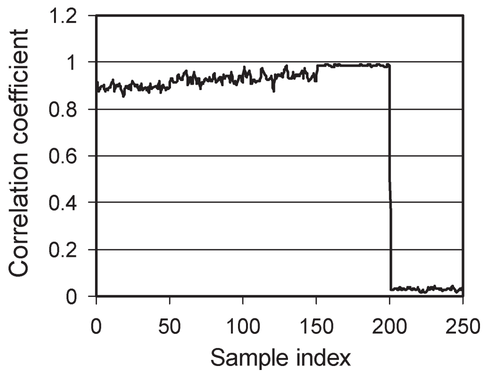

Fig. 8. Correlation coefficient between the UV-enhanced and IR signals.

2) If the flame is stable, the brightness, oscillation frequency, and correlation coefficient are high enough: around 3.3 V, 9 Hz, and 0.92, respectively.
3) In case of an unstable flame, the oscillation frequency has reduced significantly, while the correlation coefficient remains at a similar level, whereas the brightness may change depending on the extent of the instability.
4) When the flame goes out, both the brightness and the oscillation frequency are much smaller than the lower limits of their normal ranges, although the signal samples from the two cells are well correlated.
5) If the UV-enhanced cell is completely damaged, its output is almost a zero line, and the oscillation frequency calculated from each sample is meaningless and, hence, omitted in Fig. 7. In this case, the correlation coefficient between each sample from the UV-enhanced cell and the corresponding sample from the IR cell is very small.

It is clear that the five different conditions, as discussed above, have been successfully detected using the multicell flame monitor without the aid of any other self-checking mechanism.

From the results presented above, the following can be concluded.

1) If all the brightness, oscillation frequency, and correlation coefficient between any two signals are large enough, then the flame is stable; in the experiments presented earlier, these values are around 3.3 V, 9 Hz, and 0.92, respectively.
2) If both the oscillation frequency and the correlation coefficient have no major changes, but the level of the brightness goes down significantly, a sighting-tube blockage can be asserted.
3) If both the brightness and the oscillation frequency become markedly smaller, the flame is unstable. In this case, the correlation coefficient remains large.
4) If the correlation coefficient is large enough, but both the brightness and the oscillation frequency become very small [smaller than in case 3)], the flame can be considered out. In this case, the detected signal comes from the hot refractory. In a utility boiler, the detected signal may also come from the water walls and the flame skirt of the other burners.
5) If the correlation coefficient is very small and approaching zero, the cell, with a near zero brightness output, can be considered completely dysfunctional. In this case, Table I is used to pick out the dysfunctional cell.

As the three different cells are used, three separate brightness signals and three oscillation frequencies can be obtained. Apart from the self-checking and flame-failure detection, both the flame-stability monitoring and the sighting-tube-blockage detection may be achieved through the use of the three cell signals. By averaging the three brightness signals and the three oscillation frequencies, a more reliable indication of the flame stability and the working conditions of the sighting tube can be achieved. It is also worth mentioning that, if a cell develops a fault, the monitor can still work by using the remaining two cells until the monitor is repaired. This is an additional advantage of the new monitor over the conventional ones.

V. Conclusion

A new flame monitor consisting of three photovoltaic cells has been designed and implemented for the online monitoring of the combustion flames. Results arising from the experiments carried out on an industrial-scale combustion test facility have demonstrated that the new type of flame monitor can be used not only to detect the flame presence and the sighting-tube blockage but also to monitor the flame stability. The new type of monitor requires no dedicated self-checking hardware, as self-checking is implemented through the cross correlation between the signals from the three cells. The overall reliability of the multiple-cell monitor is better than the conventional single-cell detector, as it no longer suffers any abrupt failure of the self-checking hardware as well as being able to remain in operation after a cell-failure alarm has gone off. Future work will include online evaluation of the monitor on full-scale industrial boilers as well as compact design through the use of the embedded DSP hardware.

References

[1] A. R. Jones, "Flame failure detection and modern boilers," *J. Phys. E, Sci. Instrum.*, vol. 21, no. 10, pp. 921–928, Oct. 1988.
[2] A. G. Gaydon and H. G. Wolfhard, *Flames, Their Structure, Radiation and Temperature*. London, U.K.: Chapman & Hall, 1979.
[3] R. R. Beal, "New tools for safeguarding utility boiler furnaces," in *ISA Proc. 4th Nat. Power Instrum. Conf. (Instrument Society of America)*, 1961, pp. 131–140.
[4] A. W. ter Meulen, "New developments in flame detection and burner management systems for large multiburner boilers," *Flammenueberwachung-Brenne-rsteuerungen*, Haus der Technik EV. (Cambridge, MA: ECA), 1982.
[5] B. E. Noltingk, "Flame monitoring in large boilers," *Br. Combust.*, vol. 2, no. 2, pp. 4–14, 1977.
[6] A. Matsuzaki, T. Yamanaka, A. Hashimoto, *et al.*, "New products for boiler safety operation," *American Society of Mechanical Engineers (Paper), 91-JPGC-RWR-61*, pp. 1–7, 1991.
[7] P. Jackson and J. Bulger, "Enhancing techniques for flame monitoring," *Control Instrum*, vol. 19, no. 9, pp. 73–75, 1987.
[8] M. Khesin, "Demonstration of new frequency-based flame monitoring system," in *Proc. Amer. Power Conf.*, Chicago, IL, 1996, vol. 58-II, pp. 1010–1013.
[9] A. Hamins, J. C. Yang, and T. Kashiwagi, "An experimental investigation of pulsation frequency of flames," in *Proc. 24th Symp. Combustion*, 1992, pp. 1695–1702.
[10] P. M. Willson and T. E. Chappell, "Pulverised fuel flame monitoring in utility boilers," *Meas. Control*, vol. 18, no. 2, pp. 66–72, 1985.
[11] J. A. Broadbend, "Fundamental flame flicker monitoring for power plant boilers," in *Proc. IEE Semin. Adv. Sens. Instrum. Syst. Combustion Process.*, Jun. 2000, pp. 4/1–4/4.

[12] Y. Huang, Y. Yan, G. Lu, and A. Reed, "On-line flicker measurement of gaseous flames by image processing and spectral analysis," *Meas. Sci. Technol.*, vol. 10, no. 8, pp. 726–733, Aug. 1999.
[13] L. J. Xu and Y. Yan, "An improved algorithm for the measurement of flame flicker frequency," in *Proc. 21st IEEE Instrum. Meas. Technol. Conf.*, Como, Italy, May 18–20, 2004, vol. 3, pp. 2278–2281.

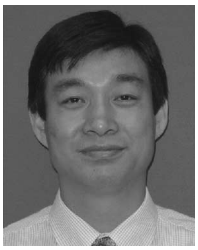

Lijun Xu (M'04–SM'04) received the B.Eng., M.Eng., and Ph.D. degrees in electrical engineering and instrumentation from Tianjin University, Tianjin, China, in 1990, 1993, and 1996, respectively.

From 1995 to 1997, he was a Lecturer and, in 1997, was an Associate Professor with the School of Electrical Engineering and Automation, Tianjin University, where he was involved in instrumentation, process control, industrial tomography, multiphase flow measurement, and signal processing. From January 2002 to December 2004, he was a Research Fellow with the University of Greenwich and the University of Kent, U.K. From December 2004 to April 2006, he was a Higher Scientific Officer with the Institute of Cancer Research, University of London, London, U.K. He is currently with the School of Instrument Science and Opto-Electronics Engineering, Beijing University of Aeronautics and Astronautics, Beijing, China. His current research interests include ultrasound measurement and imaging, process monitoring, fault diagnosis, pattern recognition, digital-signal processing, and multiphase flow measurement. He has authored and coauthored more than 80 publications.

Dr. Xu twice obtained the Deutscher Akademischer Austauschdienst (DAAD) scholarships as a visiting scholar with the University of Karlsruhe, Germany. He was a recipient of the Natural Science Award of Tianjin, the Sixth Tianjin Youth Science and Technology Award, and the Tianjin University Top-Ten Pioneer Youth Award in 2001. He has been a member of the Multiphase Flow Measurement Committee, China Metrological Measuring Institute, since 1998.

Yong Yan (M'04–SM'04) received the B.Eng. and M.Sc. degrees in instrumentation and control engineering from Tsinghua University, Beijing, China, in 1985 and 1988, respectively, and the Ph.D. degree in flow measurement and instrumentation from the University of Teesside, Middlesbrough, U.K., in 1992.

In 1988, he started his academic career as an Assistant Lecturer with Tsinghua University. In 1989, he joined the University of Teesside as a Research Assistant. After a short period of postdoctoral research, he worked initially as a Lecturer with the University of Teesside, from 1993 to 1996, and then as a Senior Lecturer, Reader, and Professor with the University of Greenwich from 1996 to 2004. He is currently a Professor with Electronic Instrumentation and the Head of the Embedded Systems and Instrumentation Research Group, University of Kent, Canterbury, U.K. He has published more than 170 research papers and has supervised ten Ph.D. research students to a successful completion. He is a Fellow with the Institute of Physics, U.K., and a Fellow of the Institute of Measurement and Control, U.K.

Dr. Yan was awarded the achievement medal by the Institution of Electrical Engineers in 2003. He is a member of four U.K. national technical committees and expert panels.